

# Self-assembled flower-like nanostructures of InN and GaN grown by plasma-assisted molecular beam epitaxy

MAHESH KUMAR<sup>1,2</sup>, T N BHAT<sup>1</sup>, M K RAJPALKE<sup>1</sup>, B ROUL<sup>1,2</sup>, P MISRA<sup>3</sup>,  
L M KUKREJA<sup>3</sup>, NEERAJ SINHA<sup>4</sup>, A T KALGHATGI<sup>2</sup> and S B KRUPANIDHI<sup>1,\*</sup>

<sup>1</sup>Materials Research Centre, Indian Institute of Science, Bangalore 560 012, India

<sup>2</sup>Central Research Laboratory, Bharat Electronics, Bangalore 560 013, India

<sup>3</sup>Laser Materials Processing Division, Raja Ramanna Centre for Advanced Technology, Indore 452 013, India

<sup>4</sup>Office of Principal Scientific Advisor, Government of India, New Delhi 110 011, India

MS received 18 March 2010

**Abstract.** Nanosized hexagonal InN flower-like structures were fabricated by droplet epitaxy on GaN/Si(111) and GaN flower-like nanostructure fabricated directly on Si(111) substrate using radio frequency plasma-assisted molecular beam epitaxy. Powder X-ray diffraction (XRD) and scanning electron microscopy (SEM) were used to study the crystallinity and morphology of the nanostructures. Moreover, X-ray photoelectron spectroscopy (XPS) and photoluminescence (PL) were used to investigate the chemical compositions and optical properties of nano-flowers, respectively. Activation energy of free exciton transitions in GaN nano-flowers was derived to be ~28.5 meV from the temperature dependent PL studies. The formation process of nano-flowers is investigated and a qualitative mechanism is proposed.

**Keywords.** Nitrides; nano-flowers; photoluminescence; RF-MBE.

## 1. Introduction

Zero-dimension and one-dimension structures of indium nitride and gallium nitride are known to have great prospects in fundamental physical science and novel technological applications (Morkoc and Mohammad 1995; Ponce and Bour 1997). Because of the large bandgap of GaN and small bandgap of InN and size confinements in such nanostructures, the fabrication of infrared, visible and ultra-violet light emitting devices (LED) with relatively low power consumption is potentially feasible (Takeuchi *et al* 1998; Matsuoka *et al* 2002; Wu *et al* 2002; Chen *et al* 2006). These studies mainly focused on zero-dimension quantum dot, one-dimensional nanowires or nanorods and two-dimensional quantum well structures. The investigation of combined zero and one-dimensional nanometre-scale InN and GaN flowers could enable unique opportunities in understanding fundamental concepts underlying the observed optical, electronic and mechanical properties. In growing pure InN and GaN, the main difficulty lies with their thermal decomposition, which becomes excessive above 500°C for InN and 800°C for GaN, and its impurity incorporation problem, especially by oxygen (Wang and Yoshikawa 2004). Plasma-assisted molecular beam epitaxy (MBE) is a suitable method for producing InN and GaN, because low

growth temperatures are possible in combination with an ultra high vacuum (UHV) growth environment, thus reducing the impurity incorporation (Lu *et al* 2001; Nanishi *et al* 2003). To fabricate III-nitride nanostructures by Stranski–Krastanow (SK) growth mode (Adelmann *et al* 2002), recently droplet epitaxy (DE) technique has been utilized (Maruyama *et al* 2007). In DE technique, to convert the droplets into semiconductor nanostructures, group III droplets are exposed to a subsequent group V molecular beam in DE–MBE approach. During this process, liquid metal droplet can be modified into various shapes of nanostructures (Lee *et al* 2009). The vapour phase growth mechanisms of nanowires include vapour–solid (VS) and vapour–liquid–solid (VLS). Contrary to the restricted growth of nanowires from the metal catalysts by VLS mechanism, the VS mechanism can give more freedom in the formation of nano-flowers.

In this study, InN nano-flowers structures on GaN/Si(111) substrates were grown by droplet epitaxy technique and GaN nano-flower structures on Si (111) substrate by VS mechanism using an RF plasma-assisted MBE.

## 2. Experimental

The growth system employed in the present study was RF-MBE system (OMICRON) equipped with a radio frequency (RF) plasma source. The base pressure in the system was below  $1 \times 10^{-10}$  mbar. The undoped silicon

\*Author for correspondence (sbk@mrc.iisc.ernet.in)

(111) wafers, as substrate, were loaded into the MBE system and out-gassed at 900°C for 1 h to remove the native oxide. Then, 250 nm of GaN films were grown directly on the substrate. After GaN growth, nitrogen plasma was switched on for 10 min at 540°C substrate temperature, forming a nitrogen rich surface. The plasma power and nitrogen flow rate were kept at 350 W and 0.7 sccm, respectively. The sample was then exposed to an indium (In) molecular beam at 160°C just above the melting point of In for 180 s. In cell, temperature was kept at 830°C and corresponding beam equivalent pressure (BEP) was  $6.7 \times 10^{-7}$  mbar. Next, the In droplets were exposed for 30 min with nitrogen plasma for nitridation of the In droplets. The nitrogen flow rate and plasma power were 0.7 sccm and 350 W, respectively. In addition, a post-growth annealing at 400°C was carried out for 30 min. This sample was labeled sample A. In sample B, after thermal cleaning of Si(111), the sample was exposed to gallium (Ga) molecular beam at 800°C for 60 s. Afterwards, nitrogen plasma and Ga flux were

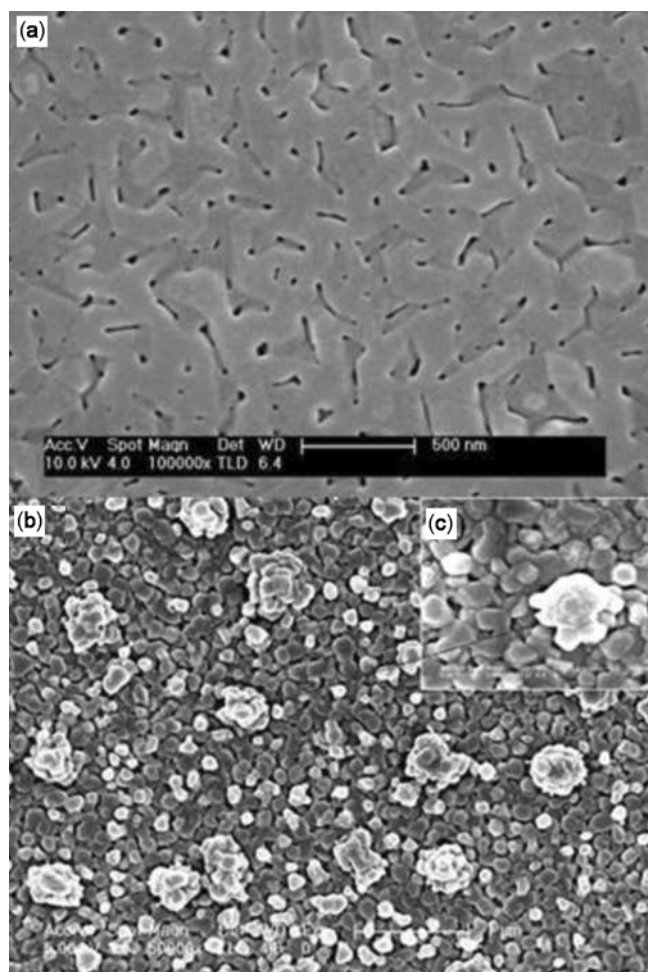
switched simultaneously for 60 min at 800°C substrate temperature, which led to the formation of GaN flower-like structures. The plasma power and nitrogen flow rate were kept at 350 W and 0.7 sccm, respectively and Ga cell temperature was kept at 950°C and corresponding BEP was  $5.6 \times 10^{-7}$  mbar.

The structural characterization, surface morphologies and chemical composition studies were carried out by XRD, SEM and XPS. Besides, the flower-like nanostructures were characterized by temperature dependent PL spectroscopy using the 325 nm line of a He–Cd laser as an excitation source.

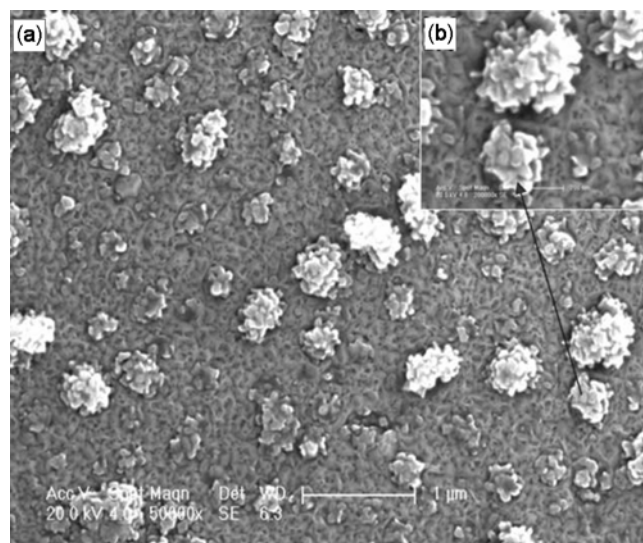
### 3. Results and discussion

Figure 1 shows the surface morphology of the GaN and as-grown InN nanostructures on the *c*-plane GaN/Si(111) substrates. From the SEM observations, it is evident that the deposited InN nanostructures have flower-like morphology, in between flowers and each flower-like nanostructure contains few leaf-like InN nanoflakes. GaN flower-like nanostructures are shown in figure 2 at different magnifications.

Figure 3 shows  $2\theta/\omega$  XRD pattern of the InN flower-like nanostructures grown on *c*-plane GaN on Si(111) and GaN flower-like nanostructures grown on Si(111) substrate. In sample A, the diffraction peaks appearing at 31.226° and 34.662° are assigned to the InN (0002) and GaN (0002) diffractions of the wurtzite-type structures, in which the peak appearing at 28.482° is due to the Si(111) diffraction. In sample B, the diffraction peak appearing at 34.662° is assigned to the (0002) diffractions of the wurtzite-type structure of GaN. In addition, the



**Figure 1.** SEM images of (a) GaN surface on Si(111) substrate, (b) and (c) InN flower-like nanostructures grown on GaN/Si(111) at different magnifications ( $\times 50000$  and  $\times 200000$ , respectively).



**Figure 2.** SEM images of flower-like GaN nanostructures grown on Si(111): (a) magnification,  $\times 50,000$  and (b) magnification  $\times 2,00,000$ .

XRD of the nanostructures also shows features typical of nanodimensional particles. The InN (0002) and GaN (0002) planes of wurtzite structures are not well defined, appearing as a broad peak, indicating the small size of particles. According to the line width analysis of the (0002) diffraction peak based on the Scherrer formula, the InN and GaN flower-like structures are on the nanometer scale and an average crystallite size of about 11.21 and 10.87 nm was roughly estimated, respectively.

The XPS spectrum was acquired using  $AlK_{\alpha}$  radiation ( $h\nu = 1486.6$  eV). Figures 4(a)–(b) show the In3d and N 1s XPS spectra of InN nano-flowers, respectively. All the binding energies were corrected with contamination C 1s signal (285.0 eV). The In3d core is spin-orbit split to the  $3d_{5/2}$  at 444.2 eV and  $3d_{3/2}$  peak at 451.7 eV. The peak at around 396.5 eV corresponds to N 1s of InN nanostructures. These results are close to the reported values of InN films (Lu *et al* 1993; Parala *et al* 2001). Figures 4(c)–(d) exhibit the binding energy peaks of Ga3d at 20.2 eV and of N1s at 397.2 eV of GaN nanostructures, respectively and these values are very close to reported values of bulk GaN (Kowalski *et al* 2001, 2004).

The optical properties of the InN nano-flowers were characterized by low temperature PL measurements. The 10 K PL spectra of InN nanostructures, as shown in figure 5(a), was found to have peak energies centred at 0.720, 0.782 and 0.852 eV. Notably, the PL spectrum contained multiple peaks and slightly blue shifted compared to the bulk InN, which may be due to the presence

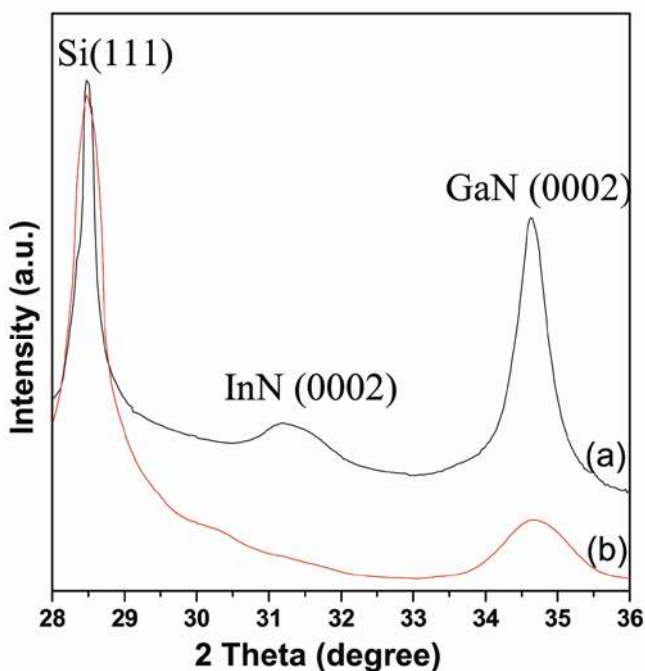
of nano families with different particle sizes in the sample and the size dependent quantum confinement effect, respectively (Brusaferri *et al* 1996). Figure 5(b) shows temperature-dependent PL spectra of GaN nano-flowers, in the range of 5–295 K. The two emission lines, observed at low temperatures below 60 K were assigned to the donor bound exciton (DBE) emission which is merged with two-electron satellites (TES) of DBE and the free exciton (FX) emission. With increasing temperature, the intensity of the DBE peak decreased abruptly due to delocalization of the bound exciton, while that of the FX peak decreased gradually with temperature. This is the typical behaviour of free and bound exciton emissions commonly observed in epitaxial GaN (Chen *et al* 2006). In addition, the FX and DBE emission peaks of GaN nano-flowers were found to be slightly blue-shifted compared to bulk GaN, which was attributed to the quantum confinement effect (Ke *et al* 2006; Park *et al* 2008) in GaN nano flowers. The decrease of PL intensity with increasing temperature can be demonstrated by the thermal ionization of electron–hole bound states or localized states. The intensities of the FX transition peaks at different temperatures have been fitted with the generalized expression (Davies *et al* 1989)

$$I(T) = I_0/[1 + C_0 \exp(-E_a/kT) + C_1 \exp(-E_{loc}/kT)], \quad (1)$$

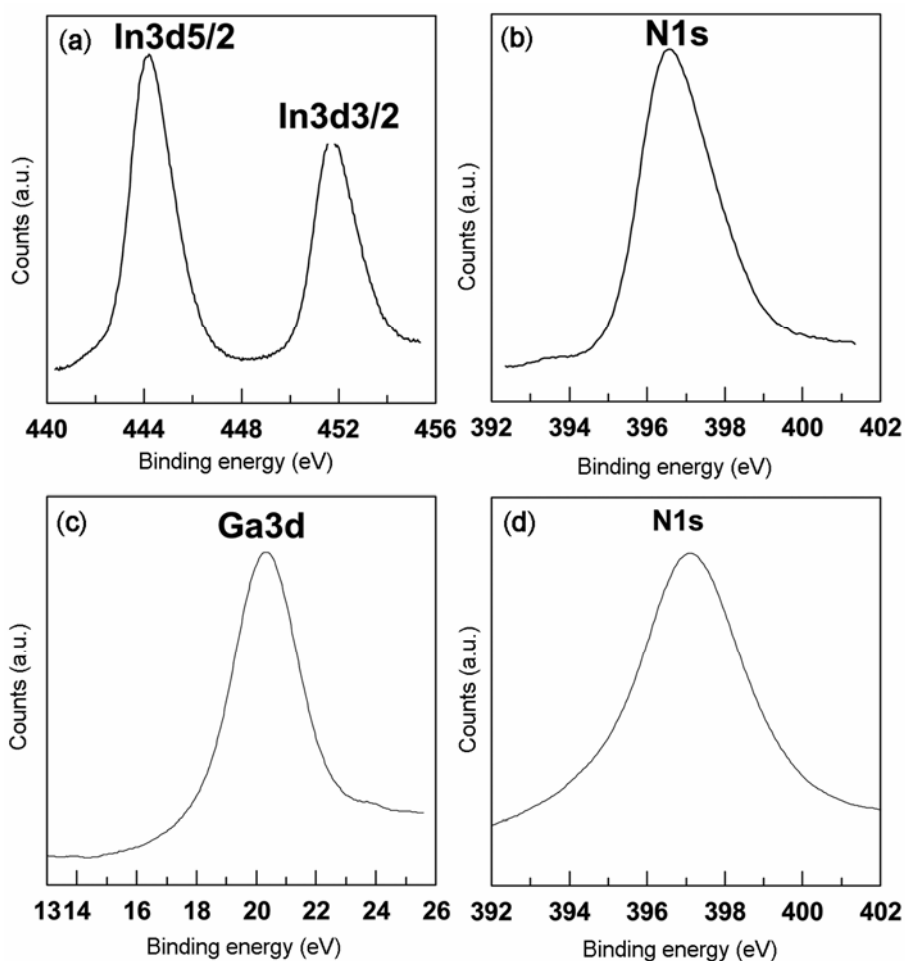
where  $I(T)$  is the PL intensity at temperature  $T$ ,  $C_0$ ,  $C_1$  and  $I_0$  are constants,  $k$  is Boltzmann's constant and  $E_a$  and  $E_{loc}$  are the activation energy and localization energy in the high and low temperature regime, respectively.

Figure 6 shows Arrhenius plot for the peak PL intensities for the FX transition related PL emission as a function of temperature. We expect the PL intensity to be dominated by localized excitons at low temperature ( $T < 60$  K). At higher temperatures ( $T > 60$  K), the PL intensity is controlled by thermally activated centres. The fit gives, localization energy ( $E_{loc}$ ) to be 5.2 meV and thermal activation energy ( $E_a$ ) to be 28.5 meV. Thermal activation energy is slightly higher than that reported by Park *et al* (2008) who reported a value of 21 meV and Chen *et al* (2006) and Chichibu *et al* (1996) who reported a value of 217 meV, perhaps due to the size dependent quantum confinement effect in the nano-flowers.

A schematic diagram of the growth mechanism of InN flower-like nanostructure is shown in figure 7. An In droplet on a planar GaN surface is shown schematically in figure 7(b). The net inward force per length applied to the drop at any point on the contact line is  $\gamma_{ls} - \gamma_{vs}$ , where  $\gamma_{vs}$  and  $\gamma_{ls}$  are the energies of the vacuum–solid and liquid–solid interfaces, respectively. (The force vector from the liquid surface tension,  $\gamma_{vl}$ , sums to zero around the contact line, and so does not contribute to the net force on the droplet.) In a symmetric situation, this inward force vector has equal magnitude around the entire perimeter, so it integrates to zero total force on the drop. The nitridation at 160°C is converting In droplets into InN but



**Figure 3.**  $2\theta/\omega$  XRD profile of the flower-like nanostructures of (a) InN grown on *c*-plane GaN/Si(111) and (b) GaN grown on Si(111) substrate.



**Figure 4.** XPS spectra of (a) In<sub>3d</sub> and (b) N<sub>1s</sub> of InN nanostructures on GaN/Si (111), (c) Ga<sub>3d</sub> and (d) N<sub>1s</sub> of the GaN nanostructures.

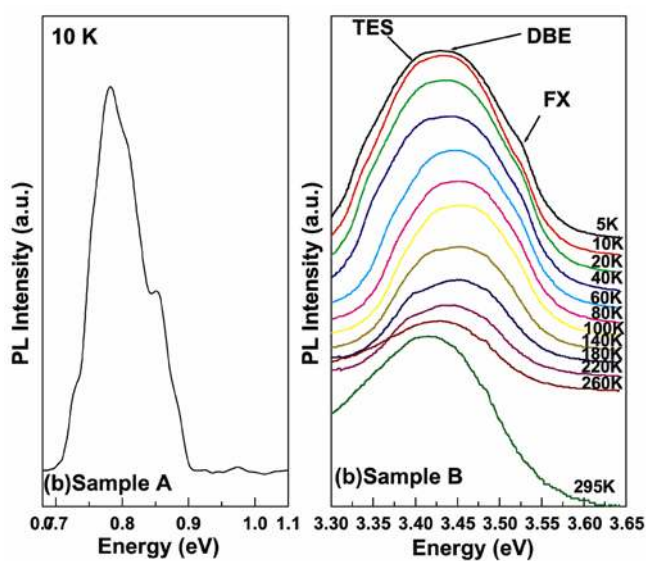


**Figure 5.** The PL spectra of the flower-like nanostructures of (a) InN grown on *c*-plane GaN/Si (111) and (b) GaN grown on Si(111) substrate.

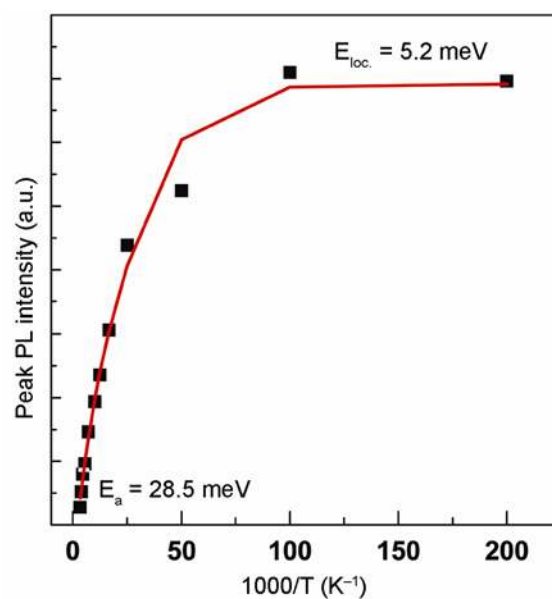


**Figure 6.** Peak PL intensities of FX transition as a function of temperature of the GaN nano-flowers.

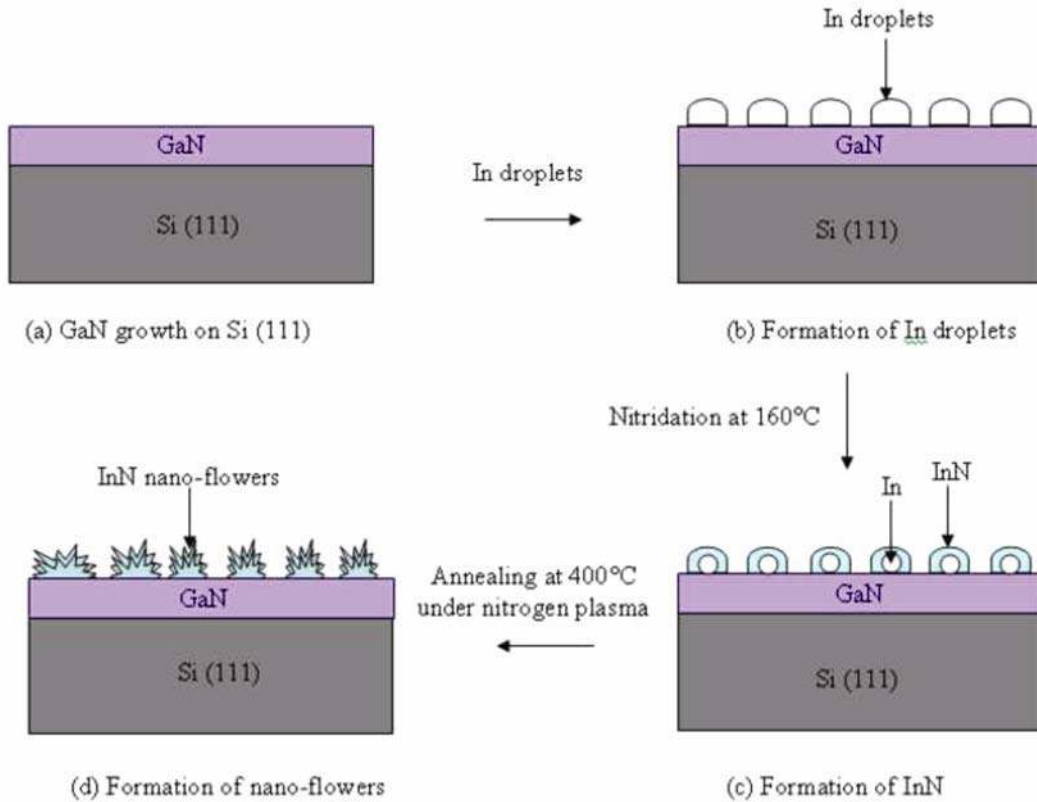


**Figure 7.** Schematic of growth mechanisms of InN nano-flowers on GaN/Si(111) substrate.

due to surface diffusion limitation, In metal is not completely converting in InN as shown in figure 7(c).

Integrating the force vector around the perimeter, the total net force on the droplet is

$$F_{\text{tot}} = (\gamma_{\text{s(InN)}} - \gamma_{\text{s(In)}})d, \quad (2)$$

where  $d$  is the droplet diameter and  $\gamma_{\text{s(InN)}}$  and  $\gamma_{\text{s(In)}}$  are the surface energies of liquid–solid interface of InN and In, respectively. If  $\gamma_{\text{s(In)}} < \gamma_{\text{s(InN)}}$ , the droplet will remain stable but if  $\gamma_{\text{s(In)}} > \gamma_{\text{s(InN)}}$ , the In will come out through InN cap layers in different shapes and minimizing the surface energy. The surface energies,  $\gamma_{\text{s(InN)}}$  and  $\gamma_{\text{s(In)}}$ , depend on temperature and above a critical temperature,  $\gamma_{\text{s(In)}} > \gamma_{\text{s(InN)}}$ . When the substrate temperature increased from 160–400°C under nitrogen plasma, above critical temperature, liquid In came out through InN cap layers in nano-flower, minimizing the surface energy. During annealing at 400°C for 30 min under nitrogen plasma, In is completely converting in InN nano-flowers which is confirmed by our XRD analysis showing only hexagonal InN diffraction patterns. The GaN nano-flowers shown in figures 2(b)–(c) could be formed by the formation of small-sized GaN seed particles first and then growth of thin nanoflakes from the seeds. Many nanoflakes from the seeds can grow into a flower structure.

#### 4. Conclusions

Self-assembled InN flower-like nanostructures on GaN/Si (111) and GaN flower-like nanostructures on Si (111) have been grown successfully by RF MBE via non-catalytic route. The possible growth mechanism of InN and GaN nano-flowers are proposed. The nano-flowers were analysed by SEM, XRD and XPS. From the PL of GaN at low temperatures, the main emission lines were assigned as DBE and FE transitions which were blue shifted, due to the size confinement effect. The activation energy of FX emission lines of GaN nano-flowers was derived to be 28.5 meV. Thus the non-catalytic route provides a simple method to grow nano-flowers and gives freedom to fabricate a variety of nanostructures compared to the catalyst-confined vapour–solid–liquid (VLS) mechanism.

#### References

- Adelmann C, Gogneau N, Sarigiannidou E, Rouviere J L and Daudin D 2002 *Appl. Phys. Lett.* **81** 3064
- Brusaferri L *et al* 1996 *Appl. Phys. Lett.* **69** 3354
- Chen H Y, Lin H W, Shen C H and Gwo S 2006 *Appl. Phys. Lett.* **89** 243105
- Chichibu S, Azuhata T, Sota T and Nakamura S 1996 *J. Appl. Phys.* **79** 2784

- Davies G 1989 *Phys. Rep.* **176** 83
- Ke W C et al 2006 *Nanotechnology* **17** 2609
- Kowalski B J, Plucinski L, Kopalko K, Iwanowski R J, Orłowski B A, Johnson R L, Grzegory I and Porowski S 2001 *Surf. Sci.* **482–485** 740
- Kowalski B J, Iwanowski R J, Sadowski J, Kowalik I A, Kanski J, Grzegory I and Porowski S 2004 *Surf. Sci.* **548** 220
- Lee J H, Wang Z M, Kim N Y and Salamo G J 2009 *Nanotechnology* **20** 285602
- Lu H, Schaff W J, Hwang J, Wu H, Koley G and Eastman L 2001 *Appl. Phys. Lett.* **79** 1489
- Lu Y, Ma L and Lin M C 1993 *J. Vac. Sci. Technol.* **A11** 2931
- Maruyama T, Otsubo H, Kondo T, Yamamoto Y and Naritsuka S 2007 *J. Cryst. Growth* **301/302** 486
- Matsuoka T, Okamoto H, Nakao M, Harima H and Kurimoto E 2002 *Appl. Phys. Lett.* **81** 1246
- Morkoc H and Mohammad S N 1995 *Science* **267** 51
- Nanishi Y, Saito Y and Yamaguchi T 2003 *Jap. J. Appl. Phys.* **42** 2549
- Parala H, Devi A, Hipler F, Maile E, Birkner A, Becker H W and Fischer R A 2001 *J. Cryst. Growth* **231** 68
- Park Y S, Kang T W and Taylor R A 2008 *Nanotechnology* **19** 475402
- Ponce F A and Bour D P 1997 *Nature* **386** 351
- Takeuchi T et al 1998 *Appl. Phys. Lett.* **73** 1691
- Wang X and Yoshikawa A 2004 *Prog. Cryst. Growth Charact. Mater.* **48/49** 42
- Wu J, Walukiewicz W, Yu K M, Ager III J W, Haller E E, Lu H, Schaff W J, Saito Y and Nanishi Y 2002 *Appl. Phys. Lett.* **80** 3967